J Mater Sci (2006) 41:8130–8137
DOI 10.1007/s10853-006-0621-7

Preparation of zirconia dental crowns via electrophoretic deposition

Christian Oetzel · Rolf Clasen

Received: 17 January 2006 / Accepted: 26 June 2006 / Published online: 4 November 2006

Abstract Tetragonally stabilized, polycrystalline zirconia (TZP) is an interesting material for dental applications due to the tooth-like appearance, biocompatibility and, compared with other advanced ceramics, high bending and tensile strength. At present fully sintered TZP dental crowns or bridges can only be made via CAD-CAM supported mechanical milling processes, but the high costs and long processing times are disadvantageous. In contrast to this process a less expensive preparation is possible via near net-shape electrophoretic shaping from aqueous suspensions and consecutive sintering. As the deposition rate for electrophoretic deposition (EPD) is independent of particle size, bimodal starting powders can be used for optimizing the green density of the compact. Thus the shrinkage during sintering can be minimized. Furthermore, the pore structure can be controlled.

In this paper the preparation of dental crowns via EPD is shown. With a combination of commercially available micron-sized Ce-stabilized zirconia (Ce-ZrO_2) powder, nanosized zirconia powder (nano-ZrO_2), and a submicron alumina powder (Al_2O_3) compacts with relative green densities up to 78% could be achieved. These compacts could be completely sintered at 1,600 °C with a linear shrinkage of less than 9%.

C. Oetzel · R. Clasen (✉)
Department for Powder Technology, Saarland University, Building D2 2, Saarbrücken D-66123, Germany
e-mail: r.clasen@nanotech.uni-saarland.de

Introduction

A lot of ceramic materials might be applied for dentures due to their tooth-like appearance (color and translucence) and biocompatibility (chemical resistance and non-toxicity) [1, 2]. Furthermore, ceramic materials show high compressive strength, low mechanical abrasion, and small thermal conductivity. On the other hand, the bending and tensile strength are problematical because high shearing stresses up to 500 MPa are observed during chewing [3]. With transformation toughened ceramics bending strengths of more than 1,000 MPa can be achieved [1, 4]. The reason for that are energy dispersive mechanisms like transformation toughening or formation and deflection of micro cracks, which are caused by the stress induced volume expansion of the tetragonally stabilized zirconia during the phase transition from the tetragonal to the monoclinic phase [4].

At present CAD/CAM processing combined with mechanical milling is established on the market for the preparation of complete ceramic dental crowns and bridges [4]. At this process the surface structure of the tooth stump is 3-dimensionally recorded at first [5]. Then a virtual crown or bridge is constructed with the CAD software. If green compacts are used for milling the shrinkage during sintering is overcompensated. With a 3 or 6 axis CAM milling machine the calculated structure is milled from a ceramic green body or an already densified (mostly additionally hipped) ceramic material. The latter is more precise with respect to geometrical dimensions, but the effort of milling these hard ceramic materials is very high. For that expensive diamond tools are needed and the working time is generally long. The milling of green compacts is much

easier, but compacts with very high homogeneity are needed to control precisely the shrinkage during sintering. The price of these CAD/CAM systems is rather high.

An alternative to these CAD/CAM processing might be the near net shaping of compacts. As the shrinkage during sintering should be small high green densities are needed. For that electrophoretic deposition (EPD) is most suited because the highest green densities compared to slip casting and other well-known ceramic shaping methods could be obtained with EPD [6]. Due to the high dielectric constant of water high deposition rates can be achieved with aqueous suspensions in contrast to suspensions based on organic liquids. Thus it was shown that deposition rates up to 1 mm/s could be reached for clay suspensions [7]. Unfortunately, problems arise with the formation of gas bubbles (O_2 and H_2) at the electrodes during EPD of aqueous suspensions, if the applied voltage lies above the decomposition voltage of water (typically 1.24 V). As these gas bubbles are incorporated into the deposited compacts leading to unacceptable holes, they have to be avoided. The membrane method [8] is one possibility to surpass these problems and has been applied for shaping of a lot of ceramic materials [9–11].

Another advantage of the EPD is that the deposition is (nearly) independent of particle size. Thus even mixtures of powders with very different particle sizes (e.g., micron and nanosized particles) are not separated [6]. Bi- or multimodal particle size distributions are necessary to obtain very green densities above 74%, which is the theoretical limit for densely packed monodisperse particles. These high green densities are needed to reduce the linear shrinkage during sintering below 10% [12]. Powder mixtures should show similar zeta-potentials of all species to prevent separation. But for concentrated suspensions this restriction is less important, because slower particles cannot be passed by faster particles with higher surface charge.

In this paper a selection of results of modifying the membrane method for the near net shaping of dental crowns from aqueous suspension of zirconia stabilized with ceria (Ce-ZrO_2) are presented. More details are given in [13]. The influence of additions of nanosized zirconia powders and submicron alumina powders on the properties of the suspensions, the EPD and final sintering of the deposited compacts was investigated. The objectives were to optimize the green density to reduce shrinkage during sintering and to stabilize the tetragonal phase of zirconia at a maximum of sintered density.

Experimental set-up

Aqueous suspensions were prepared with the starting powders zirconia stabilized with 12 mol% ceria (Ce-ZrO_2) from Vita Zahnfabrik, Bad Säckingen, a nanosized monoclinic zirconia from Degussa AG, Hanau (nano-ZrO_2), and submicron alumina from Teimei Chemicals (Al_2O_3). Typical TEM-pictures are shown in Fig. 1. The particle size distribution plotted in Fig. 2 shows medium particles diameters of 3.3 μm (BET surface area: 1 m^2/g), 50 nm (BET surface area: 56 m^2/g), and 0.15 μm (BET surface area: 14 m^2/g), respectively.

These powders were dispersed in pure water with a dissolver Dispermat N1 and, additionally, with an ultrasonic disperser. To increase the stability and improve the solids loading at a minimum viscosity the surfactant CE64® Zschimmer & Schwarz) was added. The pH-value was adjusted with tetramethyl ammonium hydroxide (TMAH). Although it is principally possible to deposit positively charged zirconia particles at low pH-values, all experiments were

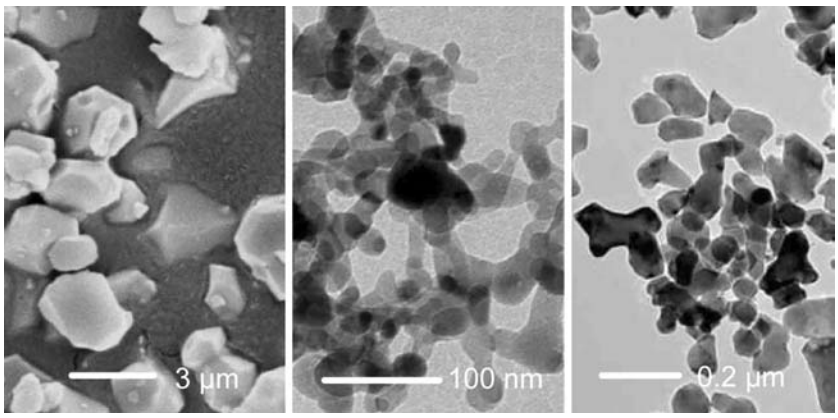

Fig. 1 Starting powders. From left to right: Ce-ZrO_2, nano-ZrO_2, and Al_2O_3

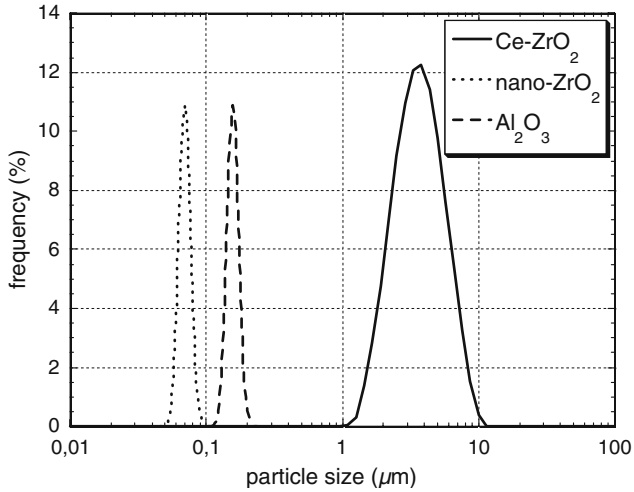

Fig. 2 Particle size distributions of starting powders

performed under basic conditions at high pH-values. The measured zeta-potentials of the monocomponent zirconia suspensions without dispersing aid are shown in Fig. 3 (Acoustosizer IIs). At acidic conditions Ce^{4+}-ions would be solved and CE64® acts better under basic conditions.

The ratio of Ce-ZrO_2, nano-ZrO_2 and Al_2O_3 was varied and the influence on the rheological properties of the suspension and green density of the EPD compacts studied. Furthermore, the addition of CE64® was changed. The viscosity of the suspension was measured with a rotational viscosimeter (Haake Rheostress).

The modified membrane apparatus for EPD is shown in Fig. 4. The anode (positive pole of the applied DC voltage) is located in the center of a drilled hole inside the porous membrane material, which is dipped in the suspension. The surrounding cathode (negative pole) can directly hold the suspension. Alternatively there can be an additional glass bottle and the shape of the cathode can be fitted to the outer shape of the membrane to control the local electric field. Thus the thickness of the deposited ceramic cap can be adjusted. The EPD of the dispersed powders takes place on the outside of the membrane, which has the shape of the dental stump. In this work models similar to typical crowns were chosen. The space between the anode and the membrane is filled with a compensation liquid of adjustable electric conductivity (typically water and TMAH). Plaster is used as the membrane material because it is a standard material for dental modeling. There are also plasters on the market, which expand during setting. Thus the shrinkage during sintering can be compensated by over sizing the deposition mold. In Fig. 5 two commercially available plasters are shown.

Typical deposition parameters were applied voltages of 6 V/cm and a ratio of 1:50 for the conductivities of suspension σ_{susp} and compensation liquid σ_{comp}. After deposition the caps were dried on the plaster. The cap was released from the mold by a controlled heating up to 500 °C, in doing so the plaster shrinks from the cap.

The pore sizes and the green density of deposited green bodies were measured by mercury porosimetry (Pascal 140 and 440) and the Archimedes method, respectively. Finally, these caps were sintered in air with different temperatures and dwelling times. The total shrinkage was measured and the phase composition of the ceramics analyzed with x-ray diffraction (XRD, Siemens D500). The green and sintered compacts were observed with a high-resolution scanning electron microscope (HRSEM, JEOL JSM-6400) on fractured surfaces.

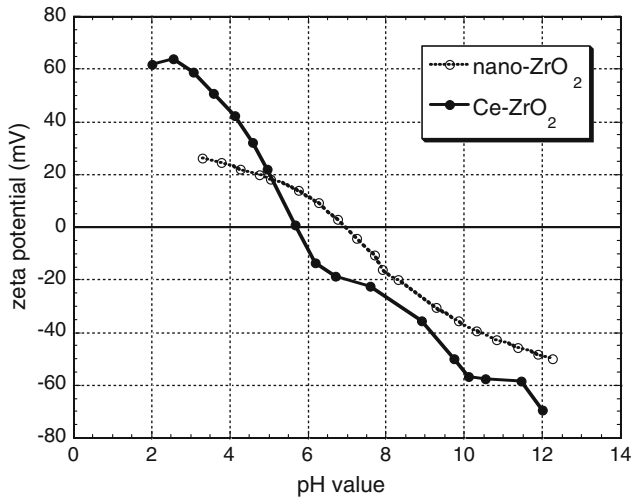

Fig. 3 Zeta potentials of the starting powders measured in aqueous suspensions

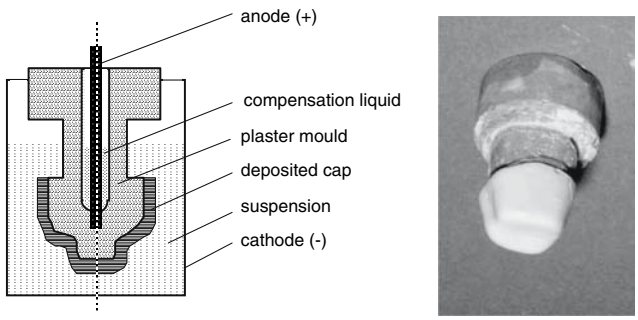

Fig. 4 Longitudinal section (schematic) of the EPD cell (left) and photograph of a deposited cap on the plaster mold (right)

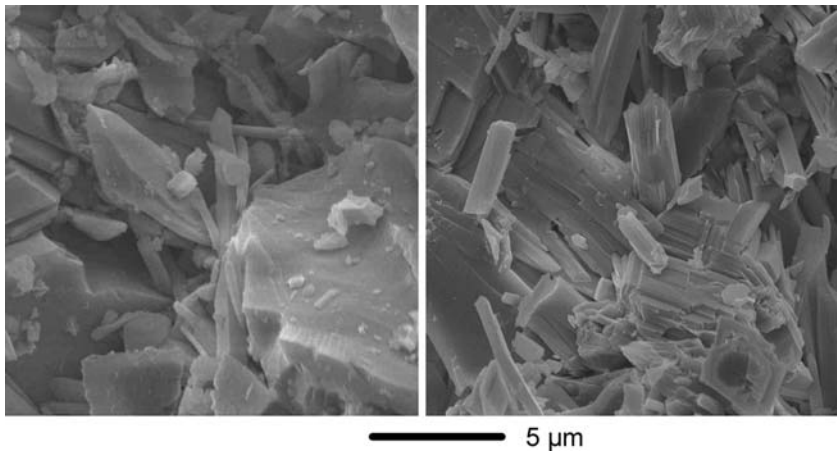

Fig. 5 SEM pictures of different plasters used as membrane material. Left Hafner expansion, right: Vita normal

Experimental results

At first the amount of additives (CE64®, TMAH) of the suspension was optimized. It is known that the viscosity should be low and, on the other hand, the solids loading should be as high as possible to reach high green densities. As it can be seen from Fig. 6, a low viscosity is observed between pH-values of 10.3 and 11.3 for an addition of 0.2 wt.% CE64® to an zirconia suspension with approx. 90 wt.% solids loading (Ce-ZrO_2:nano-ZrO_2 = 92:8). This composition was used as a standard for the following experiments. The electrical conductivity of the suspension should not exceed 1.5 mS/cm. Otherwise no EPD can be obtained. Below 0.9 mS/cm the viscosity of the suspension increased and the suspension was instable. Higher amounts of CE64® led to an increase of electrical conductivity without lowering the viscosity.

The influence of the dispersing methods is shown in Fig. 7. The green density of the EPD compact was measured for suspensions dispersed in a dissolver (2000 rpm) and an ultrasonic disperser. Obviously the dispersing of the suspension with bimodal zirconia powders in a dissolver is superior to the ultrasonic disperser, while the addition of Al_2O_3 powders reverses the situation.

After optimizing the amount of additives and dispersing conditions the optimum ratio of Ce-ZrO_2 and nano-ZrO_2 was investigated. As can be seen in Fig. 8 the maximum green density of 74.4% was obtained for 8 wt.% nano-ZrO_2. This correlates to the maximum of the solids loading in the suspension of 90 wt.%. The influence of the composition of zirconia powders on the pore size distribution of the EPD compact measured with Hg-porosimetry is shown in Fig. 9. As expected the pore sizes correlate to the particle size of the micron or nanosized powders. For powders mixtures a bimodal pore size distribution is obtained. This is not an ideal situation, but can also bee seen in the SEM pictures.

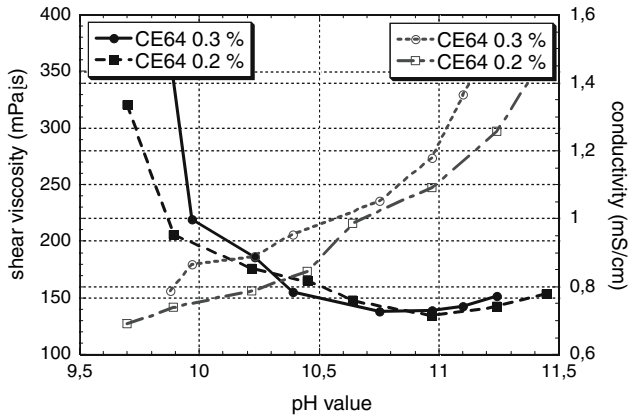

Fig. 6 Viscosity and conductivity of suspensions (92% Ce-ZrO_2 + 8% nano-ZrO_2 + CE64 + TMAH)

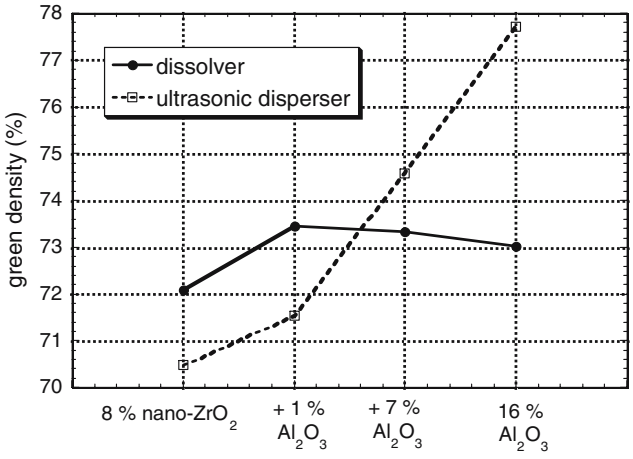

Fig. 7 Influence of alumina additions to the Ce-ZrO_2/8% nano-ZrO_2 suspension on green density (8,3 V/cm, t = 2 min, σ_{comp} = 50 mS/cm)

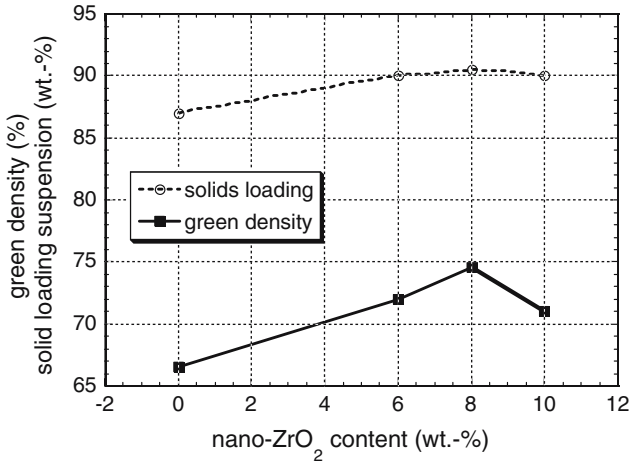

Fig. 8 Correlation of solids loading in suspension and obtained green density of the content of nano-ZrO_2 (6 V/cm, σ_{comp} = 0.2 mS/cm, t = 2 min)

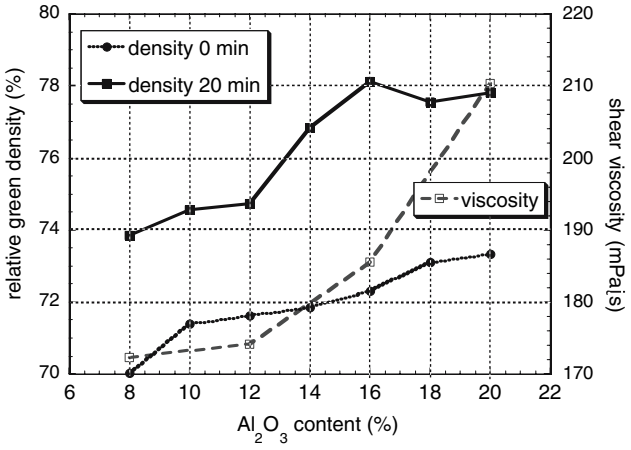

Fig. 10 Influence of the Al_2O_3 addition on the viscosity of the zirconia suspensions and green density of the EPD compacts for two kinds of dispersing

As it was observed that pure zirconia compacts showed transitions to the monoclinic phase during sintering due to grain growth, alumina had to be added to stop the growth of crystallites. Therefore the influence of Al_2O_3-additions to the zirconia suspension on the viscosity of the suspension and the green density of the EPD compact was measured. The results are shown in Fig. 10 for short dispersing by stirring (0 min) and extended dispersing in the dissolver at 2000 rpm (20 min). The advantages of the improved dispersing with the dissolver can clearly be recognized. The viscosity of 210 mPa s measured at a shear rate of 50 1/s for an addition of 20 wt.-Al_2O_3 is still acceptable. At the maximum green density of 78% with an Al_2O_3-addition of 16 wt.% a homogeneous compact is obtained, see Fig. 11. In contrast to the compact of Ce-ZrO_2 and nano-ZrO_2 shown on the left hand side the Ce-ZrO_2/Al_2O_3 compact has a unimodal pore size distribution with a maximum at 40 nm.

For all pure zirconia samples with all compositions a complete sintering to theoretical density (6.1 g/cm^3) was not possible. In all cases a at least partial transition to the monoclinic phase was observed. Only with the addition of Al_2O_3 the tetragonal phase could be stabilized at sintering temperatures up to 1,700 °C and dwelling times of 3 h. This can be seen in the XRD diagram shown in Fig. 12. At longer dwelling times a complete transition to the monoclinic phase was observed again. In Fig. 13 the sintering of two different Al_2O_3/Ce-ZrO_2 compacts is shown by plotting the linear shrinkage as a function of temperature. Additionally, the grain structure can be seen from the SEM pictures corresponding to 1700 °C (12 wt.-Al_2O_3) and 1600 °C (16 wt.-Al_2O_3). In both cases the total linear shrinkage is below 10%. At least at 1700 °C all pores have disappeared.

Finally, in Fig. 14 photographs of 3 different sintered zirconia caps are shown from 2 view positions, which are uniform along the deposition direction.

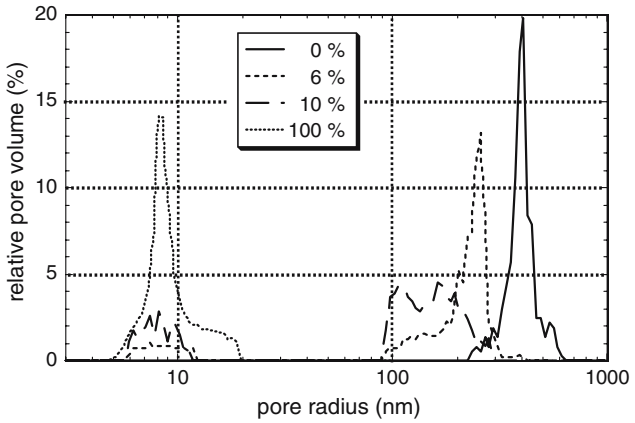

Fig. 9 Pore radius of green bodies for different contents of nano-ZrO_2

Discussion

The adaptation of the known membrane process to the EPD of near net shaped crowns could be successfully performed, even for caps with incisor shape and very tiny structures. After deposition and drying the deposited caps could be easily removed from the plaster mold after an appropriate heat treatment.

For the EPD the surface charge of the particles and the stability of the suspension are most important. The

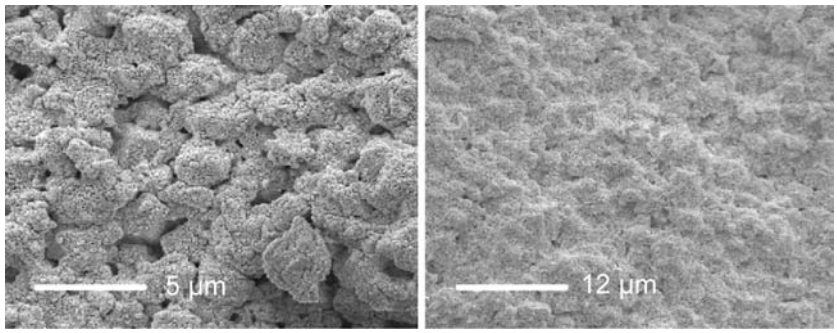

Fig. 11 HR-SEM pictures of EPD compacts. Left: Ce-ZrO_2/nano- ZrO_2 (90:10), right: Ce-ZrO_2-Al_2O_3 (84:16)

electrosteric stabilization of the suspension was superior to the pure electrostatic stabilization because higher solids loading could be obtained. As this is generally correlated to higher green densities of the deposited compacts, it was essential for reaching the objectives. For all suspensions an optimum amount of 0.2 wt.% of CE 64 was found. This is a little bit surprising because replacing Ce-ZrO_2 powder by nano-ZrO_2 or Al_2O_3 powders should increase the total free surface. One explanation might be that that the fine particles are adsorbed on the bigger Ce-ZrO_2-particles and, consequently, the surface area is only slightly increased. This can be assumed from the HR-SEM pictures. The optimum range of the pH value between 10.3 and 11.3 can be explained by increasing amount of dissociated adsorbed molecules with increasing addition of TMAH. Thus the surface charge on the particles grows and, consequently, the repulsion between particles. From a certain pH value all molecules are dissociated. Further addition of TMAH leads now to a destabilization of the suspension according to the DLVO theory.

The properties of the suspension (e.g., maximum solids loading, viscosity) depend significantly on the amount of added submicron or nanosized powders. The highest solids loading at acceptable viscosity (<200 mPa s) led to EPD compacts with the highest green density. Pure Ce-ZrO_2 suspensions show an optimum solids loading at 87 wt.%. The addition of 8 wt.% nano-ZrO_2 shifts this maximum to 90 wt.% in spite of the significantly increased total particle surface. A close look to the HR-SEM pictures let assume that the small particles partially adsorb shell-shaped on these bigger Ce-ZrO_2 particles. The other small particles remain in the suspension. Thus it is easier for the bigger particles to move under shear stress, the viscosity decreases and higher solid loadings are possible. Above 10 wt.% of nano-ZrO_2 the amount of ''free'' particles increases drastically, leading to an increase of the total free surface. Therefore the maximum solids loading decreases with an increase of viscosity. During deposition these small particles can fill up the pores between bigger particles, thus increasing the green density. But a complete filling of all pores is not possible, at least not for a bimodal system. This was shown by the measurements of the pore size distribution in the green compact.

Similar to nano-ZrO_2, the addition of Al_2O_3 also increases the maximum solids loading of the suspension up to 91 wt.% with a still acceptable viscosity. But

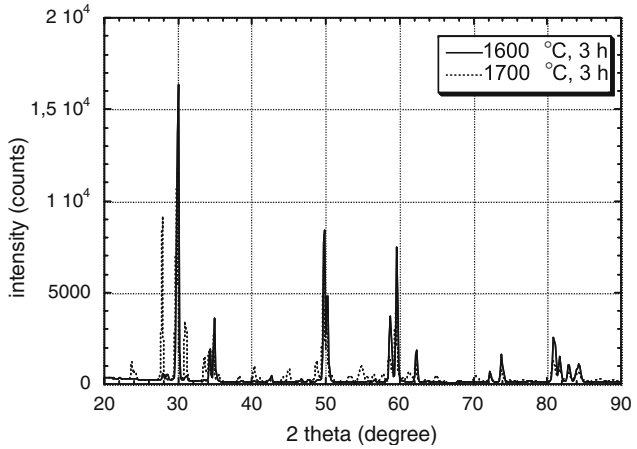

Fig. 12 XRD measurements of sintered Ce-ZrO_2/Al_2O_3 compacts (88:12)

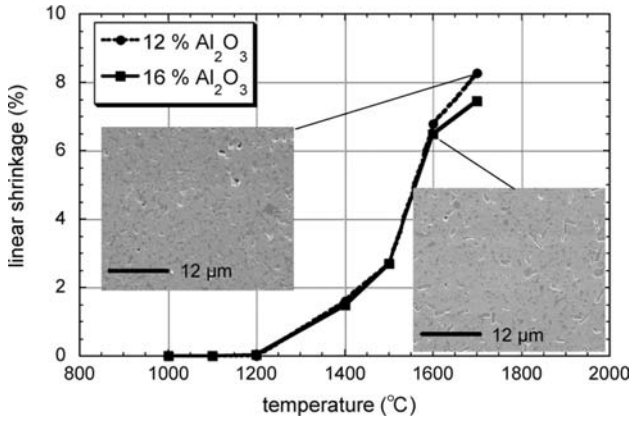

Fig. 13 Linear shrinkage during sintering of Ce-ZrO_2/Al_2O_3 EPD compacts with different compositions. Inserted are grain structures to for two temperatures

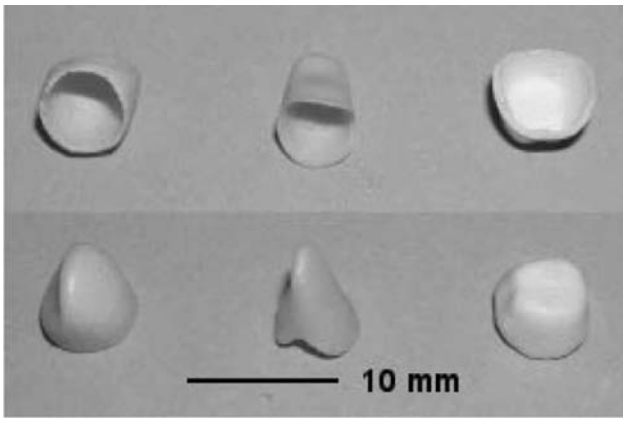

Fig. 14 Picture of sintered ZrO_2-ceramic caps

the amount that could be added, was much higher (20 wt.%). The reason for that is the much smaller surface area of the Al_2O_3 particles (14,5 m^2/g compared to 60.5 m^2/g of the nano-ZrO_2 powder). As the HR-SEM pictures showed, the pores between the bigger Ce-ZrO_2 particles could be filled up much more effectively with Al_2O_3 particles leading to a homogeneous structure with a small pore size distribution. Therefore the maximum green density was higher (78% with 16 wt.% Al_2O_3). The tendency of adsorbing on the Ce-ZrO_2 particles is smaller for the Al_2O_3 particles. Apart of the particle size the different surface properties of zirconia and alumina might explain this effect. Another evidence is given by the different dispersing behavior of the suspensions. Nanosized particles generally show a higher agglomeration rate.

It was not possible to sinter pure zirconia compacts completely to full theoretical density and to maintain the tetragonal phase. This was independent of the amount of added finer powders. The reason for that is that the critical crystallite size for the transformation from the tetragonal to monoclinic phase of the Ce-ZrO_2 particles is surpassed. The theoretical size limit is 3–4 μm. The monoclinic phase is more stable at room temperature. The addition of nano-ZrO_2 could not prevent this transformation in spite of the reduced sintering temperature with less grain growth caused by the increased green density and sinter activity of nanosized particles. The addition of yttrium stabilized nanosized zirconia powders 3Y-TZP showed no difference. But with the addition of alumina the tetragonal phase could be maintained under adapted sintering conditions. Thus a complete densification of zirconia ceramics with the tetragonal phase could be achieved at 1700 °C. At 1600 °C sintering temperature some residual pores could be still observed in the grain structure, but the densification was much higher than for the pure zirconia ceramics. The reason for that is the pinning of the grain boundaries by alumina lying at the at triple points. Thus the grain growth is slowed down, the critical crystallite size is not surpassed and the metastable tetragonal phase is maintained at room temperature. The complete transformation of the metastable tetragonal phase into the monoclinic phase at longer dwelling times (from 1 h to 4 h) supports this suggestion. The reduction of sintering temperature by 100 °C can be explained with the formation of an eutectic melt in the system CeO_2-Al_2O_3-SiO_2. Silica is expected to be present as an impurity. Taking all these fact into consideration the total linear shrinkage could be reduced to 9% and all objectives were reached.

Conclusion

Within this work the EPD membrane process was successfully adapted for the near net shaped preparation of dental crowns consisting of transformation toughened Ce-ZrO_2 ceramics. It was shown that plasters used in the dental preparation are well suited as a membrane and can be easily shaped in the desired way. The EPD compacts are deposited as caps on the outside of this shaped membrane. During the optimization of additives to improve the properties of the suspension it was shown that the electrosteric dispersing aid CE 64 is most effective in concentrations of 0.2 wt.% in the pH-value range from 10.3 to 11.3. With the addition of nanosized zirconia powders the solids loading and the green densities of the EPD compacts could be improved. The optimum was reached for 8 wt.% nano-ZrO_2 in the suspension leading to a green density of 74.8%.

For stabilizing the tetragonal phase during sintering the addition of alumina was very effective. With the addition of 20 wt.% Al_2O_3 the maximum solids loading of 91 wt.% with an acceptable viscosity of <200 mPa s was achieved. Furthermore, a green density of 78% was reached. In contrast to the bimodal zirconia powders a unimodal pore structure was found. With this addition of alumina, which pins the grain boundaries and reduces grain growth, the tetragonal phase could be maintained during sintering at temperatures up to 1700 °C. The total linear shrinkage during sintering could be reduced to 9%.

References

1. Kappert HF, Krah M (2001) Quintessenz Zahntechnik 27:668
2. Tinschert J, Natt G, Spiekermann H (2001) Dent Labor 9:293

3. Setz J, Schwickerath H (1999) In: Koeck B (ed) Kronben- und Brückenprothetik. Urban & Fischer, p 410
4. Green DJ, Hannink RHJ, Swain MV (1989) Transformation toughening of ceramics, 232nd edn. CRC Press, Boca Raton, Florida
5. Witkowski S (2003) Zahntechn Mag 6:696
6. Tabellion J (2004) Herstellung von Kieselgläsern mittels elektrophoretischer Abscheidung und Sinterung, Dissertation, Universität des Saarlandes, Saarbrücken
7. Hector I, Clasen R (1997). Ceram Eng Sci Proc 18:173
8. Clasen R (1988) In: Hausner H, Messing GL, Hirano S (eds) 2nd Int. Conf. on Powder Processing Science, Berchtesgaden, 12–14. 10. 1988: Deutsche Keramische Gesellschaft, Köln, p 633
9. Oetzel C, Clasen R (2003). Ceram Eng Sci Proc 24:69
10. Clasen R, Tabellion J (2003). cfi/Ber DKG 80:E40
11. Oetzel C, Clasen R., Tabellion J (2004). cfi/Ber DKG 81:E35
12. Zhang C, Liu D, Mathews SA, Graves J, Schaefer TM, Gilbert BK, Modi R, Wu H-D, Chrisey DB (2003) Microelectronic Engin 70:41
13. Oetzel C (2005) Herstellung vollkeramischer Zahnkronen aus Zirkonoxid und Zirkonoxid-Aluminiumoxid mit Hilfe der elektrophoretischen Abscheidung, Dissertation, Universität des Saarlandes, Saarbrücken